

Rapid #: -17960013

CROSS REF ID: **5785098**

LENDER: **COF :: Morgan Library**

BORROWER: **LUU :: Main Library**

TYPE: Article CC:CCG

JOURNAL TITLE: Advanced engineering informatics

USER JOURNAL TITLE: Advanced Engineering Informatics

ARTICLE TITLE: Robustness analysis framework for computations associated with building performance models and immersive virtual experiments

ARTICLE AUTHOR: Chokwitthaya, Chanachok,

VOLUME: 50

ISSUE:

MONTH:

YEAR: 2021

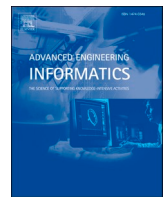
PAGES: 101401-

ISSN: 1474-0346

OCLC #:

Processed by RapidX: 9/8/2021 9:50:38 AM

This material may be protected by copyright law (Title 17 U.S. Code)



Robustness analysis framework for computations associated with building performance models and immersive virtual experiments



Chanachok Chokwitthaya ^{a,*}, Yimin Zhu ^a, Supratik Mukhopadhyay ^b

^a Department of Construction Management, Louisiana State University, Baton Rouge 70803, USA

^b Department of Electrical Engineering and Computer Science, Louisiana State University, Baton Rouge 70803, USA

ARTICLE INFO

Keywords:

Building performance model
Human-building interaction
Immersive virtual environment
Generative adversarial network
Robustness analysis
Uncertainty
Sensitivity

ABSTRACT

Building performance models (BPMs) have been used to simulate and analyze building performance during design. While extensive research efforts have made to improve the performance of BPMs, little attention has given to their robustness. Uncertainty is a crucial factor affecting the robustness of BPMs, in which such effect needs to be quantified through a suitable approach. The paper offers a robustness analysis framework for BPMs by using perturbation techniques to simulate uncertainty in input datasets. To investigate the efficacy of the framework, a generative adversarial network (GAN)-based framework was selected as a case study to analyze light switch usages in a single-occupancy office simulated using an immersive virtual environment (IVE). The robustness of the GAN was analyzed by comparing differences between a baseline (i.e., a BPM obtained from the GAN trained on a non-perturbed dataset) and BPMs obtained from the GAN trained on perturbed datasets. Overall, the robustness of the GAN significantly reduced when the training datasets were perturbed by using structured transformation techniques. The GAN remained relatively robust when the training datasets were perturbed by using an additive perturbation. Additionally, the sensitivity of the GAN involves different magnitudes corresponding to different levels of perturbed input datasets. The study suggests that the perturbation analysis is effective for investigating data uncertainty affecting the robustness of BPMs.

1. Introduction

Energy used in buildings has been cited as a major source of carbon emissions in many research studies [1–3]. Massive investments have put in commercial and residential projects, which continuously shape sustainability of future built environments (e.g., controlling carbon emissions, energy uses, and occupant comfort). Sustainable building has become one of the major contributions in building designs, involving several assessments of building factors and occupants such as energy system efficiency, material performance, lifecycle cost, and occupants' satisfaction and health [4]. Building performance models (BPMs) are decision-support tools that designers often use for understanding, analyzing, and comparing different design options to satisfy building goals and objectives [5,6]. A number of studies have developed BPMs for enhancing building performance optimizations from whole buildings

[7] to specific building systems (e.g., space heating [8], air quality [9], light switches [10], blinds, windows, and thermostats [11]). Several methods and algorithms have been used, which may be categorized in two groups, namely expert-based and simulation-based optimizations [12]. The expert-based optimization is based on a design of an experimental approach to optimize building performance without creating mathematical and/or statistical models [12]. The simulation-based optimization is mainly an automated process relying on numerical and mathematical optimizations. It has been widely accepted as the effective approach to construct BPMs [12,13]. According to the simulation-based optimization, BPMs are mostly embedded in computational processes, where they take given inputs (e.g., occupancy schedules, environmental conditions, and building materials) to analyze and estimate outputs (e.g., building performance and usages of building components) [14]. Such computations involve many sources of uncertainty such as input pa-

* Corresponding author.

E-mail addresses: cchokw1@lsu.edu (C. Chokwitthaya), yimin.zhu@lsu.edu (Y. Zhu), supratik@csc.lsu.edu (S. Mukhopadhyay).

rameters [15,16] and computational structures [17]. If the uncertainty of input parameters is too large, the computations may not be robust and generate uncertain, inaccurate, and unreliable outputs [18]. Furthermore, the computations may involve instability and faulty algorithm, which can be another factor introducing uncertainty during computational processes [19]. The robustness analysis helps to understand impacts of such uncertainty, thereby gaining more confidence in using the computations for decision-making, and, optimally, improve performance of building design and contributes to sustainable building [20].

Robustness analysis in this study is defined according to the robust theorem as investigation whether the performance of a computation remains robust and produces reliable outputs, when it is challenged by uncertainty [21]. In general, uncertainty can be classified under two heads, namely aleatory and epistemic uncertainties [22]. Aleatory uncertainty occurs due to the naturally variability of a model system. It is also known as irreducible uncertainty and is often ignored in robustness analyses. Epistemic uncertainty arises due to absence of knowledge and information in analyses. It can be reduced, if more information can be acquired [23]. For example, it may occur due to uncertainty related to the input parameters. Sources of such uncertainty may be data errors, varying degree of reliability of data collection tools, and random nature of participants. Accordingly, this work focuses on the robustness analysis of computations affected by the epistemic uncertainty.

Performing the robustness analysis requires knowledge of uncertainty of input parameters. Traditionally, data uncertainty are quantified through variations of obtained data and the variations are acquired by, for instance, repeating experiments [24]. However, many experiments, particularly experiments associated with immersive virtual environments (IVEs), cannot be repeated because of limited resources, such as times, costs, and humans [25]. Uncertainty estimations are among common strategies to mitigate the limitation and have appeared in various research fields, especially machine learnings. Two outstanding approaches are widely used to simulate uncertainty, namely Bayesian and non-Bayesian approaches [26,27]. The Bayesian approach requires prior probability distributions over input datasets to estimate posterior probability distributions through several alternative Bayesian inferences (e.g., Laplace approximation [28], variational inference [29], Markov Chain Monte Carlo [30], and Monte Carlo dropout [31]). Then, the posterior probability distributions decompose uncertainty into computational models. The approach involves approximations of prior and posterior probability distributions, which may not be suitable for computations included in BPMs, especially BPMs involving datasets associated with human interactions. Since human interactions are vulnerable to many factors and change from time to time, estimating uncertainty corresponding to human interactions through probability distributions may be inaccurate. On the other hand, the non-Bayesian approach avoids estimations of probability distributions. Among various methods, a perturbation method has been successfully used to estimate uncertainty of input parameters for robustness analyses in several studies, including image classifications [32,33], general classifications [34], and speech recognitions [35,36]. There are many types of perturbation techniques, such as adding data noise, replacing data with random ones, and altering data. To analyze the robustness, computations run on perturbed input datasets, each of which represents a different level of uncertainty. The robustness is assessed by comparing baselines (e.g., outputs generated by using non-perturbed datasets) with outputs generated by using perturbed input datasets.

The study contributes to a robustness analysis corresponding to impacts of uncertainty on computations, an important issue discussed in previous studies [15–18]. Extending to those studies, the robustness analysis for computations associated with BPMs and human-building interactions in IVEs is provided, where, moreover, uncertainty arising from such applications can be quantified. The authors experimented and investigated performance of the robustness analysis through a case study. The case study analyzed the robustness of a computation in a framework for augmenting BPMs proposed by Chokwitthaya et al. [37], in which it has been proven to appropriately construct BPMs during design. It involves an IVE, an existing BPM, and a Generative Adversarial Network (GAN), that consists of a pair of Artificial Neural Network (ANN)s playing a game with each other. Chokwitthaya et al. [37] used an IVE to simulate a new design and acquire *context-aware design-specific data* through human-building interactions. The GAN used *context-aware design-specific data* to bias an *existing BPM* (i.e., a BPM constructed by using data of human-building interactions in an existing building) toward a new design guided by a given *performance target*.

2. Robustness analysis

2.1. Introduction

The goal of the robustness analysis in this study is to determine whether a computation of a BPM produces resilient outputs. If a computation for particular assumptions about variability in inputs (e.g., uncertainty) produces similar outputs, it is considered robust for those assumptions. That is, the robustness analysis framework (Fig. 1) identifies whether a computation remains robust, when input datasets are uncertain. It determines differences between a baseline, an output generated by a computation taking a non-perturbed input dataset ($A_{non-perturbation}$), and an output generated by a computation taking a perturbed input dataset ($A_{perturbation}$). If $A_{perturbation}$ is not significantly different from $A_{non-perturbation}$, the computation is considered robust. Accordingly, the hypothesis was defined as follows:

$$H_0: A_{perturbation} \text{ is not significantly different from } A_{non-perturbation}$$

$$H_1: A_{perturbation} \text{ is significantly different from } A_{non-perturbation}$$

It has to be noted that, a baseline, in the framework, is information that users provide as a base for determining robustness of a BPM. The baseline may be obtained from both local and global analyses depended on available and appropriate baseline used in a study. It can be provided in various forms such as an average and a specific outcome of the BPM.

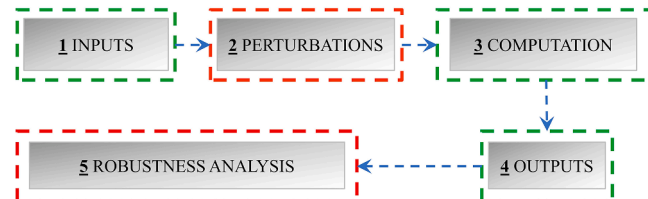


Fig. 1. The robustness analysis framework.

2.2. Perturbation

The general purpose of perturbations is to simulate variability of input datasets. In this paper, the authors use perturbations to add uncertainty to input distributions represented by their respective input datasets [38]. Perturbations may be performed using several techniques depended on types of input parameters and purposes of studies. In image classification using machine learning, common perturbation techniques include injecting noise to images [39], changing information of images (e.g., watermarking, patching, and changing pixels) [40], and transforming image geometry [41,42]. In speech recognition using machine learning, perturbation techniques include adding noisy signal [43], making speech reverberated [44], and adding background noise [45]. Other examples of perturbations are inserting sentences in question answering systems [46] and using perturbation scale to alter data [47,48].

Perturbation techniques may be categorized as an additive perturbation (e.g., injecting noise to images, adding noisy signal, and adding background noise) and a structured transformation (e.g., changing information of images, transforming image geometry, and making speech reverberated) [49]. The former adds additional unrelated data such as data noise to training datasets; whereas the latter replaces data in training datasets with unrelated data or alters data in training datasets. The two categories serve different purposes on simulating uncertainty and are meaningful in investigating and analyzing robustness of a computation.

In addition, selection of the perturbation techniques depends on parameter types and circumstances that may introduce uncertainty to parameters. For instance, IVE experiments cannot simulate or include all possible scenarios occurring in the world. Excluded scenarios may implicitly influence uncertainty of input datasets and impact robustness of a computation. Adding data noise is an alternative to simulating additional uncertainty caused by existence of excluded scenarios. Furthermore, human decisions such as choices of switching a light on or off may be subjective or even involve wrong decisions, causing uncertainty in obtained datasets. Such uncertainty can be simulated by replacing parts of input datasets with unrelated data. Another example is that sensors used in experiments may involve uncertainty caused by unreliable measurements, which can be simulated by altering datasets associated with the measurements.

Determining which variables to perturb is among key factors in the robustness analysis. It is possible that the analysis does not need to consider all variables. Although there is no specific criterion to select variables, the decision is mainly based on needs of a particular application. For instance, categorical variables (e.g., names and labels) are less likely to be subjected to uncertainty. Such variables may be excluded from being perturbed.

Levels of perturbation are important factor in the robustness analysis. They help to investigate robustness of a computation responding to different levels of uncertainty. Generally, there is no standard or rule to define the levels. Most of previous studies defined the levels based on assumed amounts of uncertainty in variables that are believed to have an impact on their computations' robustness. For instance, Haghnegahdar and Raazavi [48] used perturbation scales (e.g., $\pm 1\%$, $\pm 5\%$, $\pm 10\%$, and $\pm 20\%$) to distort datasets associated with input parameters and simulate uncertain input parameters for analyzing the robustness of earth and environmental system models.

2.2.1. Perturbation forms

2.2.1.1. Additive perturbation. An additive perturbation has been widely involved in analyzing robustness of machine learning models [50–53]. It maintains input data and adds additional unrelated data (e.g., data noise) to datasets. Its main purpose is to allow investigations whether models have ability to remain robust by maintaining the knowledge of input datasets and adding different levels of perturbation [54]. For instance, Rolnick et al. [55] investigated the robustness of their deep neural network across different levels of added noise in the perturbed training datasets. They added noise up to 100 data for every training datum in several experiments.

Adding data noise is a traditional technique of additive perturbation. One of the common noise categories is additive white Gaussian noise (AWGN), where data noise are drawn from a Gaussian (i.e., normal) distribution, which has been applied to many experimental datasets [56]. Furthermore, AWGN allows direct control over variance of noise. Data noise is generated using Gaussian (i.e., normal) distribution according to variances of input datasets, as a result, the data noise has similar variances and comparable to the input datasets. Therefore, adding AWGNs is potentially an additive perturbation technique for analyzing robustness of computations.

2.2.1.2. Structured transformation. A structured transformation (e.g., an imperceptible perturbation) investigates the robustness of models by reducing or distorting the knowledge of input datasets. It has been applied in several robustness analyses. For example, Liu et al. [57] generated perturbed input datasets of traffic signs by scrawling and patching the signs to reduce knowledge gained from the original datasets of the signs. They re-trained the classification model to investigate its accuracy. They found that the accuracy of the model decreased, which explicitly revealed decrease of its robustness. Engstrom et al. [42] distorted information of images by randomly rotating the images between -30 and $+30$ degree and transforming the images up to 10% of image pixels. Their results suggested that small rotations and transformations could significantly degrade accuracy and robustness of classifier models. Accordingly, the structured transformation is taken as one of the techniques to assist the robustness analysis in this work.

3. Case study

Fig. 2 shows the scheme and components of the GAN-based framework attached with the robustness analysis. In the following, a summary of the GAN-based framework and the IVE experiment are provided, where the complete documentation of the framework has been published in Chokwitthaya et al. [37]. Then, the robustness analysis is discussed.

3.1. The GAN-based framework

The GAN-Based Framework was proposed by the authors for augmenting BPMs [37,58]. It uses a nonparametric approach to generate a mixture model of an *existing BPM* and *context-aware design-specific data*. The framework can automatically determine an appropriate mixture by using a *performance target* as a guide. Its performance has been proven and evaluated [37]. The framework contributes to assisting and improving building performance estimations for non-existing buildings (e.g., buildings under design). There are five major components

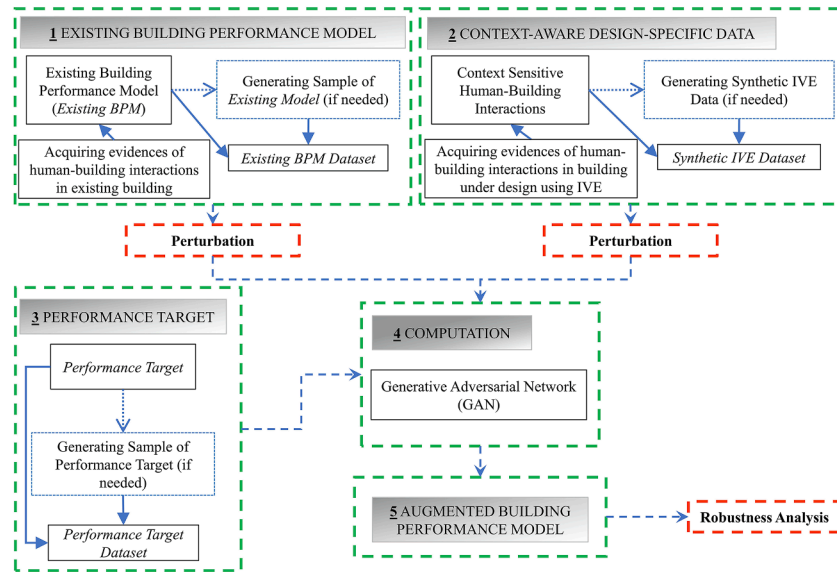


Fig. 2. GAN-based framework attached with the robustness analysis.

involved in the GAN-based framework (the green boxes in Fig. 2) including: (1) an *existing BPM*, (2) *context-aware design-specific data*, (3) a *performance target*, (4) the GAN, and (5) an *augmented BPM*.

3.1.1. Existing building performance model

An *existing BPM* describes relationships of historical events (e.g., building environments and building characteristics) and observations (e.g., human-building interactions). Traditionally, data used to construct the *existing BPM* is acquired from human-building interactions with embedded contexts of existing buildings. Consequently, the *existing BPM* may not address important contextual factors influencing human-building interactions in the context of a building under design. If the *existing BPM* is used to estimate performance of a specific space (e.g., building under design), discrepancy between estimated and actual building performance may arise.

3.1.2. Context-aware design-specific data

Context-aware design-specific data describes human-building interactions influenced by contextual factors of a specific space (e.g., a building under design). For example, the Hunt model [59] uses work area illuminance as an independent variable to predict statuses of light switch usages. However, other factors may also influence light switch usages such as office tasks (e.g., reading, relaxing, meeting, and drafting) and locations of a light switch (e.g., a switch is by a door and on a desk). For the Hunt model, the office tasks and the locations of a light switch are contextual factors, since they are not included in the model. Immersive virtual environments (IVEs) can be used to acquire such *context-aware design-specific data* [60–62].

3.1.3. Performance target

A *performance target* is a performance metric (e.g., energy intensity of a space) defined to satisfy the objectives of a building design [37]. Such performance metric is converted into operational measures for computational purposes. Nevertheless, the conversion method is still an open topic requiring further attentions. The performance target is used to guide the combination of an *existing BPM* and *context-aware design-specific data*, so that the GAN can produce an *augmented BPM*, whose analytic results are as close to the target as possible.

3.1.4. Computation

The generative adversarial network (GAN) [63] is implemented as the computation method in the framework [37]. The GAN comprises a

generator and a discriminator. The generator employs ANN to learn mixed probability distributions (i.e., mixture of an *existing BPM* and *context-aware design-specific data*) and generate an *augmented BPM* that follow a target distribution. The discriminator employs another ANN to discriminate an *augmented BPM* and the target distribution. The GAN uses the concept of a two-player minimax game to train the generator and the discriminator.

3.2. Robustness analysis of the GAN

The analysis focused on understanding the robustness of the GAN and testing the hypothesis. The estimations of light switch usages in a single-occupancy office were used as an application case. It needs to be noted that the case study reused data, and the application to obtain the data was fully reported in Chokwitthaya et al. [37]. To avoid unnecessary repetition, this section only provides a brief introduction of the major components, e.g., the *existing BPM*, the *context-aware design-specific data*, the *performance target*, the computation, and the *augmented BPM*. The training datasets associated with the *existing BPM* and *context-aware design-specific data* were perturbed by using the aforementioned perturbation techniques. *Augmented BPMs* generated by the GAN trained on the perturbed training datasets were used to analyze the robustness of the GAN.

3.2.1. Overview of the reused application

The light usage prediction model of Hunt [59] (Fig. 3) and Da Silva et al. [64] (Fig. 4) were selected as the *existing BPM* and the *performance target*, respectively. Both models described relationship between work area illuminance as an independent variable and probability of

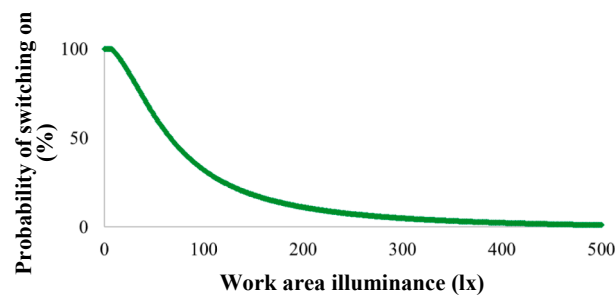


Fig. 3. Hunt model.

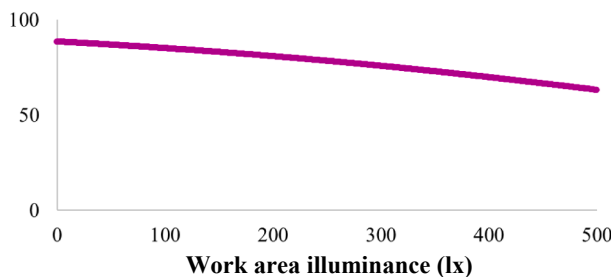


Fig. 4. Da Silva model.

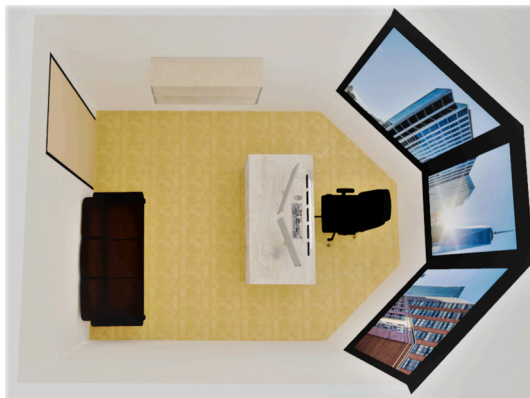


Fig. 5. Top view of the virtual office.

Table 1
Variables and their values considered in the IVE experiment.

Contextual factor		Independent variable	Dependent variable
Office task	Light switch location	Work area illuminance (lx)	Probability of switching on
Intensive reading	By the door	50	Very unlikely
Having a break	On the desk	100	Not likely
Having a meeting		150	Neutral
Drafting		200	Likely
		350	Very likely
		500	
<i>Total = 4</i>	<i>Total = 2</i>	<i>Total = 6</i>	<i>Total = 5</i>

switching on as a dependent variable. The datasets generated from the Hunt and Da Silva model were called “the *existing BPM dataset*” and “the *performance target dataset*”, respectively.

An immersive virtual environment (IVE) simulated a single-occupancy office (Fig. 5) and acquire *context-aware design-specific data* corresponding to contextual factors. The contextual factors considered in the IVE experiment were office tasks (e.g., intensive reading, having a break, having a meeting, and drafting) and light switch locations (e.g., by the door and on the desk). Similar to Hunt and Da Silva model, the independent and dependent variables included in the IVE experiment were the work area illuminance (lx) and the probability of switching on, respectively. Table 1 summarizes the contextual factors, independent, and dependent variables considered in the IVE experiment along with their values. Data corresponding to the contextual factors, independent, and dependent variables were acquired from 30 students including 18 males and 12 females and called “the *IVE dataset*”. Fig. 6 illustrates the virtual environment, when a participant was exploring the IVE and selecting probability of switching on. As discussed by Chokwitthaya et al. [25], the Gaussian mixture model (GMM) [65] was used to increase the number of independent and identically distributed (IID) samples based on the *IVE data* and generate a new dataset, called “the *synthetic IVE dataset*”.

In data preprocessing, the *existing BPM dataset*, the *synthetic IVE dataset*, and the *performance target dataset* were standardized. The *existing BPM dataset* and the *synthetic IVE dataset* were split into training datasets and testing datasets with a 70–30 split, namely the *existing BPM training dataset*, the *existing BPM testing dataset*, the *synthetic IVE training dataset*, and the *synthetic IVE testing dataset*.

The GAN comprised of a generator and a discriminator. The generator took the *existing BPM training dataset* and *synthetic IVE training dataset* as the input datasets. Before training the GAN, the generator was pre-trained on the combination of the *existing BPM training dataset* and the *synthetic IVE training dataset* to initialize its weights and biases. In every epoch, the generator gained knowledge by learning mixtures of the *existing BPM training dataset* and *synthetic IVE training dataset* and made a prediction. The prediction that was closest to the *performance target* was considered as an *augmented BPM*. The discriminator determined differences between the prediction of the generator and the *performance target dataset*. The discriminator sent a feedback to the generator for improving its knowledge of mixtures and prediction in the next epoch.

3.2.2. Perturbation

The GAN as the computation of the GAN-based framework acquired its knowledge through training datasets associated with the input

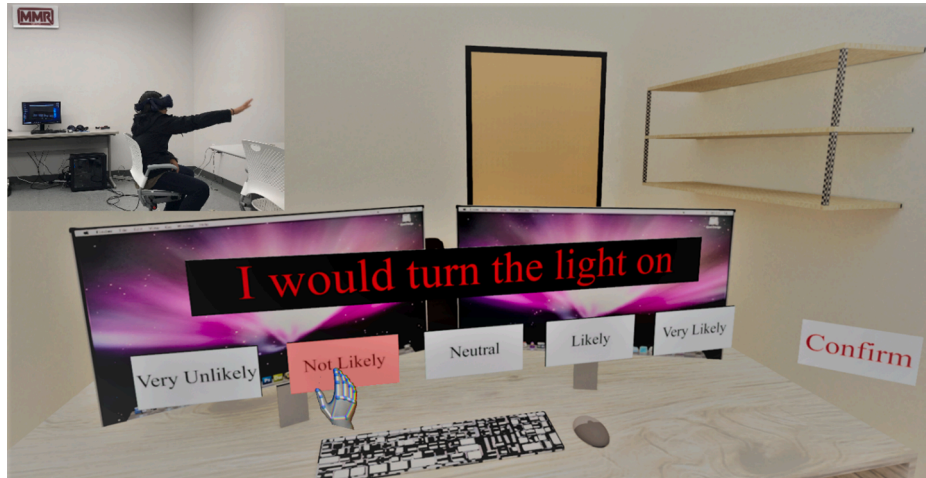


Fig. 6. A participant exploring the IVE and selecting likelihood of switching on.

Table 2

Summary of parameters and their corresponding components.

Parameter	Training dataset associated with the parameter	Variables in the training dataset subject to uncertainty	Perturbation		
			Additive perturbation	Structured transformation	
				Adding data noise	Replacing probability of switching on with random data
Existing BPM	Existing BPM training dataset	Probability of switching on Work area illuminance	Yes Yes	Yes No	No Yes
Context-aware design-specific data	Synthetic IVE training dataset	Probability of switching on Work area illuminance	Yes Yes	Yes No	No Yes

parameters. To analyze the robustness of the GAN, perturbations had to be executed on the training datasets to make them uncertain. The performance target guided the mix of two input parameters of the GAN, namely the *existing BPM* and the *context-aware design-specific data*. Although the performance target could be perturbed in theory, there was no practical meaning in the scope of this study. It was assumed that the target was specific without uncertainty.

In the case study, the contextual factors (i.e., the office tasks and the locations of the light switch) were categorical variables. Even if there was uncertainty associated with them, the impact of uncertainty was reflected through the dependent variable (i.e., the probability of switching on). Therefore, they were not included in the perturbation. On the other hand, the probability of switching on and the work area illuminance were subject to uncertainty. The former was subject to uncertainty because its data were obtained from human-building interactions, which tended to be sensitive to building contexts. The latter was subject to uncertainty because it was measured using sensors for creating the *existing BPM* and simulated using the IVE to generate the *context-aware design-specific data*. Those experimental tools and simulations often involved levels of uncertainty. Consequently, the authors perturbed data of the work area illuminance and the probability of switching on in the training datasets.

Using additive perturbation, the authors simultaneously perturbed the data of the probability of switching on and work area illuminance by adding data noise. It allowed the authors to investigate and compare overall impacts of uncertain parameters, i.e., the *existing BPM* versus *context-aware design-specific data* on the robustness of the GAN. Using structured transformation, the authors perturbed the two variables separately using two techniques, namely replacing the probability of switching on with random data and altering the work area illuminance. It allowed the authors to further investigate the impact of uncertainty of individual variables on the robustness of the GAN under specific circumstances. Table 2 summarizes the parameters used in the case study along with their corresponding training datasets, variables subject to uncertainty, and the perturbation technique applied to each variable. The perturbed training datasets were called “*perturbed existing BPM training datasets*” and “*perturbed synthetic IVE training datasets*”, when the *existing BPM training dataset* and the *synthetic IVE training dataset* were perturbed, respectively. Here, a note is put to mention that the particular design and administration of the perturbation are merely for understanding and demonstrating the impact of uncertain parameters and variables in the case study. Other applications may implement different designs and administrations depending on their purposes.

3.2.2.1. Additive perturbation. A major benefit of using the additive perturbation is to investigate whether the GAN has ability to remain robust, when the GAN maintains knowledge of training datasets associated with the *existing BPM* and the *context-aware design-specific data*,

Table 3

Ratios of adding AWGN to data in perturbed training datasets.

Case	Ratio of data in training datasets to AWGN
1	10:1
2	10:3
3	10:5
4	10:7
5	10:10

even if the perturbed training datasets contain different levels of the additive perturbation. Another benefit of using the additive perturbation is to explore whether the training datasets are sufficiently effective for the GAN to remain robust. If the GAN becomes non-robust when the training datasets involve a certain level of perturbation, revisions to the training datasets may need to be considered such as acquiring more knowledge by conducting additional experiments to enhance the efficacy of the training datasets and robustness of the GAN.

To investigate the robustness of the GAN, additive white Gaussian noise (AWGN) was added to the data of the probability of switching on and work area illuminance in the *existing BPM training dataset* and the *synthetic IVE training dataset*. The simulation of AWGN implemented the Gaussian (i.e., normal) distribution with zero means and specified variances ($N(0, \sigma^2)$) to randomly generate the noisy data. The case study used the variances of the probability of switching on and the work area illuminance as the variances of the Gaussian distribution, when adding noise to their respective data. The authors added various amount of AWGN to the training datasets as shown in Table 3. For instance, the ratio of 10:1 denoted there were 10 actual datapoints to 1 AWGN in every 11 datapoints of the perturbed datasets. The perturbation ratios were defined by considering limited resources (e.g., computational costs, and times) and purposes of the study. The application preserved the actual data as the majority in the perturbed training datasets by limiting the ratio of the actual data to AWGN at 1:1. In other applications, more perturbation ratios may be used in analyses. However, trade-off between resources needed and levels of perturbation ratios should be considered.

3.2.2.2. Structured transformation. The main contribution of structured transformation is to inspect how reduced or distorted knowledge of training datasets impacts the robustness of the GAN. It perturbs the training datasets by using two techniques for different purposes. To investigate the robustness due to the uncertain probability of switching on, portions of the training datasets with respect to the probability of switching on were replaced with random data. To analyze the robustness on uncertain work area illuminance, the data with respect to the work area illuminance in the training datasets were altered using perturbation scales. In each perturbation technique, different levels of perturbation were assigned.

3.2.2.2.1. Replacing probability of switching on with random data. Ideally, the selection of the perturbation technique reflects practical circumstances causing uncertainty in the training datasets. For instance, a participant has different preferences at different times when interacts with a light switch even if the lighting conditions were the same. The circumstance introduces uncertainty to the probability of switching on. The structured transformation is appropriate to simulate such uncertain preferences, because it replaces a portion of the probability of switching on in the *existing BPM training dataset* and the *synthetic IVE training dataset* with unrelated data. Thus, it reduces the knowledge of the training datasets. The robustness of the GAN was investigated in terms of the ability of the GAN to maintain robust, even though its knowledge of the probability of switching on was reduced in the training datasets.

In the case study, the data respecting to the probability of switch on in the training datasets were randomly replaced with random numbers between 0 and 1, where the limit based on the nature of probability. According to Table 4, three perturbation ratios (i.e., 9:1, 7:3, and 5:5) were used to replace data of the probability of switching on in the *existing BPM training dataset* and the *synthetic IVE training dataset*. For instance, the ratio of 9:1 denoted there were 9 actual data points to 1 randomized data point in every 10 data points in the perturbed datasets. The selection of perturbation ratios was dependent on mainly purposes of the study and consideration of resource limitations (e.g., computational costs, and times). The purpose of using different ratios was to assess the robustness of the GAN with respect to different amount of knowledge about the probability of switching on in the training dataset. The application preserved the actual data as the majority in the perturbed training dataset by limiting the ratio of the actual data to replaced data at 1:1 (i.e., 5:5 in Table 4).

3.2.2.2.2. Altering work area illuminance. In general, work area illuminance is subjected to uncertainty. Data of work area illuminance is often obtained from experimental tools (e.g., illuminance sensors and IVE simulations). The tools may involve uncertainty (e.g., $\pm 10\%$ of actual illuminance) and propagate the uncertainty to measured data.

In the case study, the IVE simulated illuminance levels according to analysis from a lighting simulation software (e.g., 3D Max). A method to access uncertainty of the IVE on lighting simulation has not existed. That is, the specific uncertainty associated with lighting in IVE could not be quantified. For lighting sensors used in the *existing BPM*, Hunt did not report specifications of the particular sensors and their uncertainty. Consequently, the authors did not have information about uncertainty of the sensors, and did not quantify specific uncertainty of particular sensors. Since the framework is generic, “what if” scenarios to assume such uncertainty were applied to understand possibility of different levels of uncertainty. To investigate the robustness of the GAN due to uncertainty of the work area illuminance, the authors altered data of the work area illuminance in the training datasets using perturbation scales. The technique was based on the concept of the structured transformation and adaption of previous perturbation techniques, namely transforming image geometric in Engstrom et al. [42] and using perturbation scales in Haghnegahdar and Raazavi [48]. Consequently, the perturbation scales (i.e., $\pm 10\%$, $\pm 30\%$, and $\pm 50\%$) were used to alter data of the work area illuminance in the training datasets. The perturbations were performed

Table 4

Ratios of changing data of the probability of switching on to random data in perturbed training datasets.

Case	Ratio of actual data to changed data
1	9:1
2	7:3
3	5:5

according to Equation (1). Even though, the scale of 50% may appear to be impractical, it helps to assess the robustness of the GAN regarding extreme conditions of data error. For instance, the illuminance sensors were interrupted by external signals resulting in extreme errors in the measurements. The application used a perturbation interval at 20% and limited the perturbation at 50% because of resource limitations.

$$\text{Altered illuminance} = \text{illuminance} \pm (\text{illuminance} \times \text{perturbation scale}) \quad (1)$$

3.2.3. Criteria of robustness analysis, hypothesis testing, and sensitivity investigation

The one-at-a-time (OAT) technique [66,67] was applied to train the GAN using one perturbed training dataset a time. A total of 23 *augmented BPMs* (i.e., non-perturbation + (5 cases of adding data noise + 3 cases of Replacing Probability of Switching on with Random Data + 3 cases of Altering Work Area Illuminance) * 2 input parameters) were generated.

The two-sample Kolmogorov-Smirnov test (*K-S test*) [68], a statistical test measuring a distance of two empirical distributions, was applied to test the hypothesis. A level of significant at $\alpha = 0.05$ was applied to investigate the statistically significant difference between a baseline, an *augmented BPM* generated by the GAN taking a non-perturbed input dataset ($A_{\text{non-perturbation}}$), and an *augmented BPM* generated by the GAN taking a perturbed input dataset ($A_{\text{perturbation}}$). On one hand, $P\text{-values} \leq 0.05$ indicated significant difference between $A_{\text{non-perturbation}}$ and $A_{\text{perturbation}}$ and, as a result, the GAN became non-robust. On the other hand, $P\text{-values} > 0.05$ indicated no significant difference between $A_{\text{non-perturbation}}$ and $A_{\text{perturbation}}$ and, therefore, the GAN remained robust.

Additionally, the *K-S statistic* obtained from the *K-S test* was used to assess sensitivity of the GAN. To determine the sensitivity of the GAN, pairwise comparisons of the *K-S statistic* across $A_{\text{perturbation}}$ generated from the GAN trained on the *perturbed existing BPM training dataset* and the *perturbed synthetic IVE training dataset* within the same level of perturbation were analyzed. For instance, if the *K-S statistic* associated with $A_{\text{perturbation}}$ generated from the GAN trained on the *perturbed existing BPM training dataset* and the *synthetic IVE training dataset* at 10:1 perturbation ratio was lower than that from the GAN trained on the *existing BPM training dataset* and the *perturbed synthetic IVE training dataset*, the GAN was less sensitive to the *existing BPM* than the *context-aware design-specific data*.

4. Results and discussions

Results and discussions are organized in three sections, 1) non-

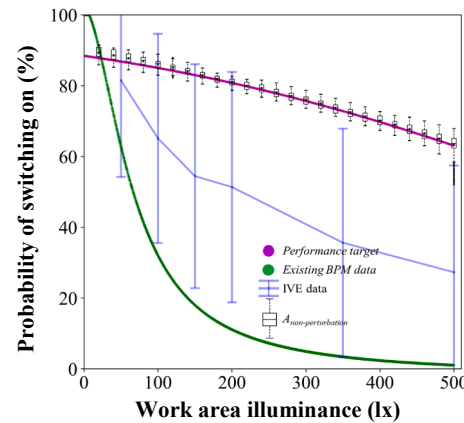


Fig. 7. An Augmented BPM corresponding to non-perturbed training dataset.

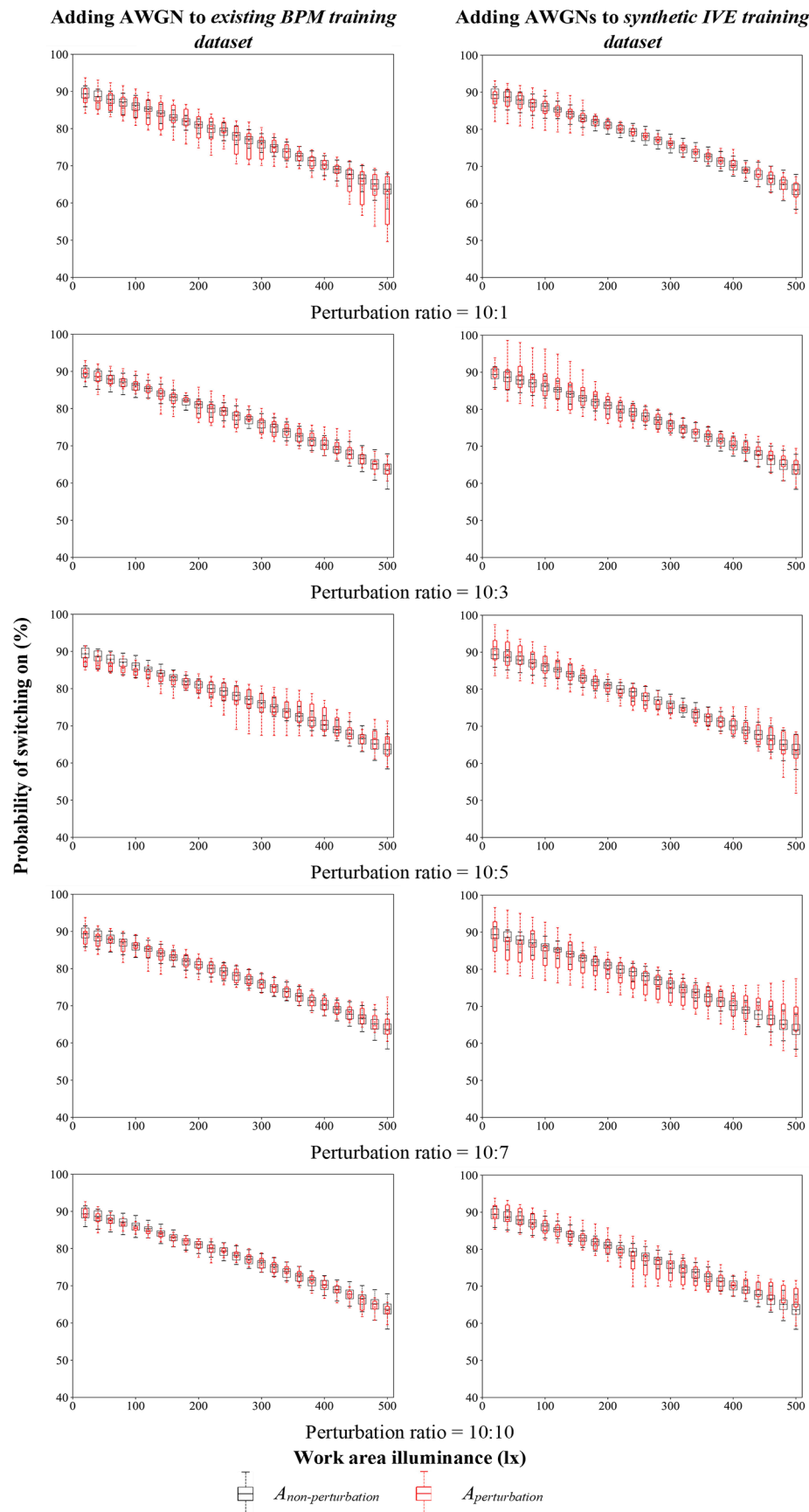


Fig. 8. Augmented BPMs corresponding to adding data noise.

perturbations, 2) additive perturbation performed by adding data noise, and 3) structured transformation performed by replacing the probability of switching on with random data and altering the work area illuminance.

Fig. 7 illustrates the $A_{\text{non-perturbation}}$, the *existing BPM training dataset*, the *performance target dataset*, as well as means and standard deviations of the *synthetic IVE training dataset* through a plot of the probability of switching on versus their corresponding work area illuminance. Figs. 8, 10, and 12 demonstrate comparisons between $A_{\text{non-perturbation}}$ and $A_{\text{perturbation}}$ corresponding to each perturbation and its levels. In Figs. 7, 8, 10, and 12, boxplots are used to demonstrate the variances representing the uncertainty of $A_{\text{non-perturbation}}$ and $A_{\text{perturbation}}$. Tables 5–7 summarize the *p-values* used to statistically evaluate the robustness of the GAN. Figs. 9, 11, and 13 show plots of *K-S statistic* associated with the levels of perturbation in each perturbation case for assessing the sensitivity of the GAN.

4.1. Non-perturbation

Fig. 7 shows the efficacy of the GAN for generating an *augmented BPM* (i.e., $A_{\text{non-perturbation}}$) that reach the performance target. According to the boxplots, uncertainty existed in $A_{\text{non-perturbation}}$, even though the input parameters were not perturbed. The finding agreed with the fact that uncertainty always exists in building performance models mentioned in literatures [20,69]. Several factors may contribute to the occurrence of uncertainty such as the nature of the GAN (i.e., aleatory uncertainty), the structure of the GAN, and the completeness of the input parameters. Such factors may need attention in future research. Additionally, the $A_{\text{non-perturbation}}$ was used as a baseline in the robustness analysis throughout the case study.

4.2. The additive perturbation

4.2.1. Adding data noise

Fig. 8 illustrates comparisons of $A_{\text{non-perturbation}}$ and $A_{\text{perturbation}}$ with respect to adding data noise to the probability of switching on and the work area illuminance. AWGN was added according to the perturbation ratios described in Table 3, i.e., 10:1, 10:3, 10:5, 10:7, and 10:10. Fig. 8 reveals that the uncertainty of $A_{\text{perturbation}}$ is slightly higher than that of $A_{\text{non-perturbation}}$, since variances in the boxplots associated with $A_{\text{perturbation}}$ are larger than those associated with $A_{\text{non-perturbation}}$. The results suggest adding noise marginally influenced the uncertainty of $A_{\text{perturbation}}$. Adding noise to the *existing BPM* seems to cause less uncertainty to $A_{\text{perturbation}}$ than adding noise to the *synthetic IVE training dataset*.

The influences of adding noise do not significantly impact the robustness of the GAN since *p-values* are greater than 0.05 in all cases as shown in Table 5. Therefore, the GAN remained robust, when the training datasets were perturbed by adding data noise at all perturbation ratios and in both cases (i.e., the *perturbed existing BPM training datasets*

Table 5

P-values corresponding to adding data noise.

Perturbation ratio	<i>Existing BPM training dataset</i>		<i>Synthetic IVE training dataset</i>	
	P-value	P-value	P-value	P-value
10:1	0.793		0.532	
10:3	0.221		0.628	
10:5	0.545		0.362	
10:7	0.545		0.059	
10:10	0.112		0.180	

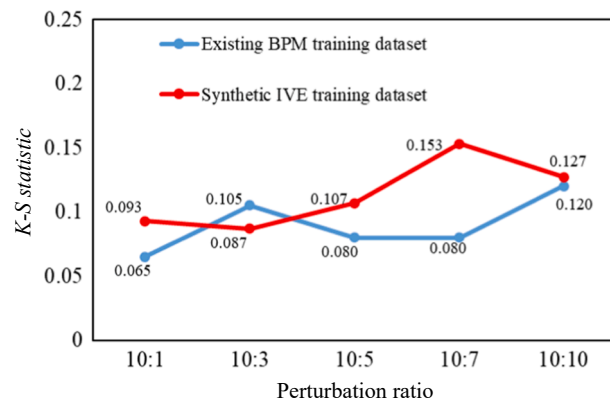


Fig. 9. K-S statistics corresponding to adding data noise.

and the *perturbed synthetic IVE training datasets*). The results suggest that as long as the original knowledge of the training datasets was intact in the training datasets, the GAN was able to remain robust, even if the level of noise was increased to 100%.

According to the *K-S statistics* reported in Fig. 9, the pattern of *K-S statistics* is not consistent across the perturbation ratios. Hence, it was unclear whether the GAN was more sensitive to the *existing BPM training dataset* or the *synthetic IVE training dataset*. Consequently, the GAN was not more sensitive to the *existing BPM* or the *context-aware design-specific data* when the training datasets were perturbed by adding data noise.

Overall, the results indicate that the GAN was able to recognize and capture underlying knowledge of the input parameters contributing to generating the *augmented BPMs* that met the performance target. The finding greatly agrees with previous studies regarding to the robustness analysis by adding data noise. For instance, Hosseini et al. [51] found that the application programming interface (API) remained robust, whose outputs for restored images largely matched that for actual ones without the need for improving the image analysis algorithm, even when noise were applied to the images. The finding, as well, agrees with Munir [70]. Munir analyzed the robustness of the selective image encryption algorithm, where adding data noise was one of the case studies. He stated that the algorithm could decrypt images effectively, when images were corrupted with various noise categories (e.g., Gaussian noise, Poisson noise, salt and pepper noise, and speckle noise).

4.3. The structured transformation

4.3.1. Replacing the probabilities of switching on with random data

The comparisons of $A_{\text{non-perturbation}}$ and $A_{\text{perturbation}}$ with respect to replacing the probability of switching on with random data between 0 and 1 are illustrated in Fig. 10, where the perturbation ratios (i.e., 9:1, 7:3, and 5:5) indicated the levels of perturbation.

Fig. 10 shows that variances increase when the perturbation ratio increases, indicating increases of uncertainty of $A_{\text{perturbation}}$. The observation implied that changing the probability of switching on in the training datasets with random data obviously contributed to the increases of uncertainty of $A_{\text{perturbation}}$ in all perturbation ratios and the training datasets. Uncertainty of $A_{\text{perturbation}}$ tended to increase in parallel with increasing the perturbation ratios and perturbing the *synthetic IVE training dataset* appeared to be more influence on the uncertainty of $A_{\text{perturbation}}$ than perturbing the *existing BPM training dataset*.

Results of the hypothesis testing presented in Table 6 unveil that when the perturbation ratio increases, the rejected cases of the null

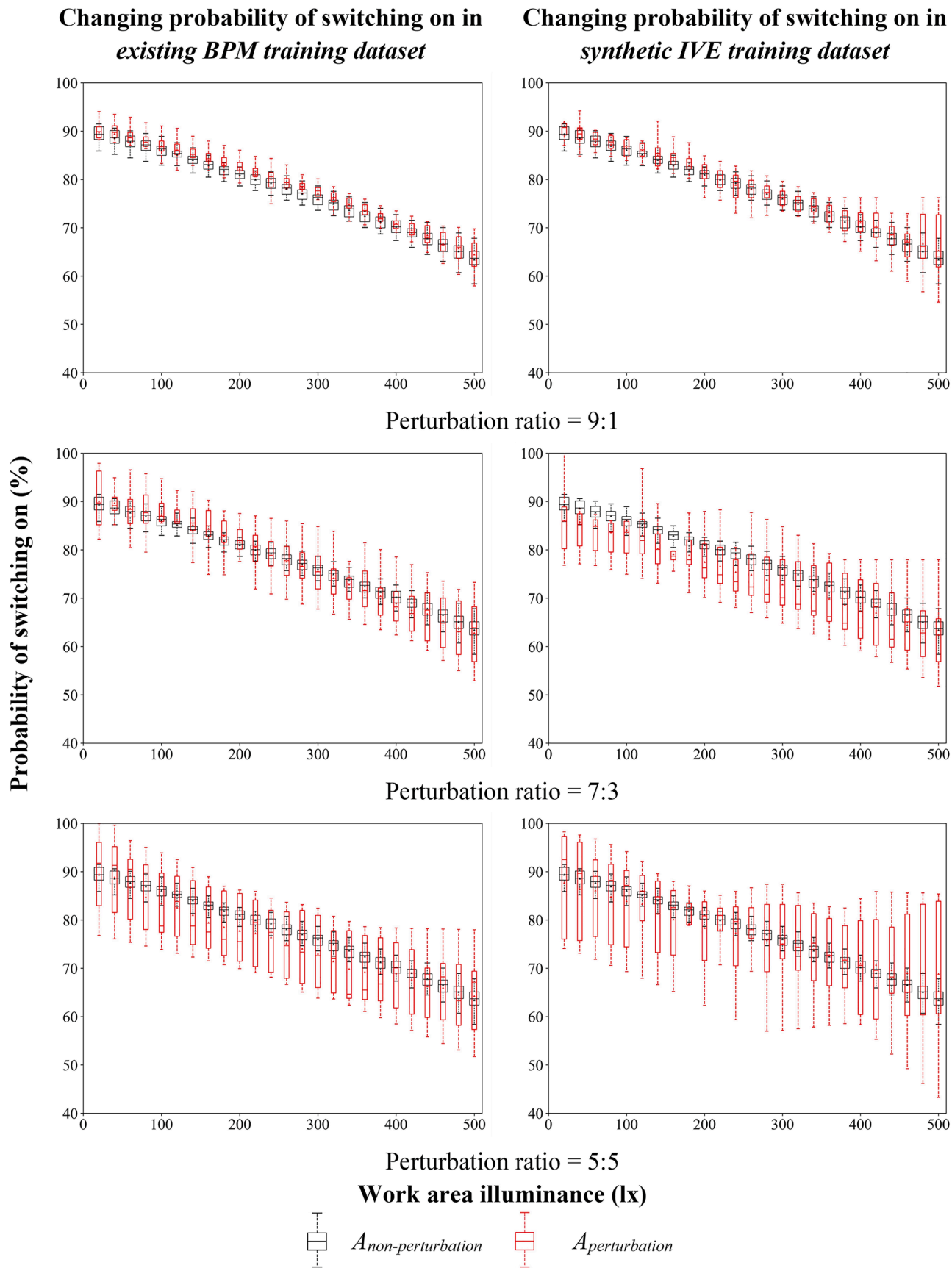


Fig. 10. Augmented BPMs corresponding to replacing probability of switching on with random data.

Table 6

P-values corresponding to replacing probability of switching on with random data.

Perturbation ratio	<i>Existing BPM training dataset</i>	<i>Synthetic IVE training dataset</i>
	<i>P-value</i>	<i>P-value</i>
9:1	0.394	0.177
7:3	0.270	<0.05
5:5	<0.05	<0.05

hypothesis ($p\text{-value} < 0.05$) increase. They suggested replacing data in the training datasets with random number reduced the level of knowledge in the GAN about the training datasets, and, thus, reduced the performance of the GAN, leading to decreases of its robustness. According to Table 6, when the probability of switching on in the *existing BPM training dataset* was perturbed, the null hypothesis was rejected in one case where the perturbation ratio was set to 5:5. However, the null hypothesis was rejected in two cases, when perturbing the same variable in the *synthetic IVE training dataset*. In other words, even though the increases of perturbation ratios reduce the robustness, perturbing the probability of switching on in the *existing BPM training dataset* has less contribution to the reduction of the robustness than perturbing that in the *synthetic IVE training dataset*.

According to Fig. 11, the *K-S statistics* associated with the *perturbed existing BPM training datasets* are lower than those associated with the *perturbed synthetic IVE training datasets* in all perturbation ratios. It implied that the GAN was less sensitive to the *existing BPM* than the *context-aware design-specific data* when the data of the probability of switching on were replaced by random data.

According to the results, meaningful discussions can be made in the following:

- When the perturbation ratio increased, the robustness of the GAN decreased and uncertainty of $A_{\text{perturbation}}$ increased. The situation occurs because replacing data in the datasets with random number contributed to reductions of actual data in the datasets. As a result, underlying knowledge of the datasets used to train the GAN was decreased. Accordingly, training the GAN by using reduced knowledge datasets reduced performance of the GAN, leading to decreases of the robustness and increases of uncertainty of $A_{\text{perturbations}}$.

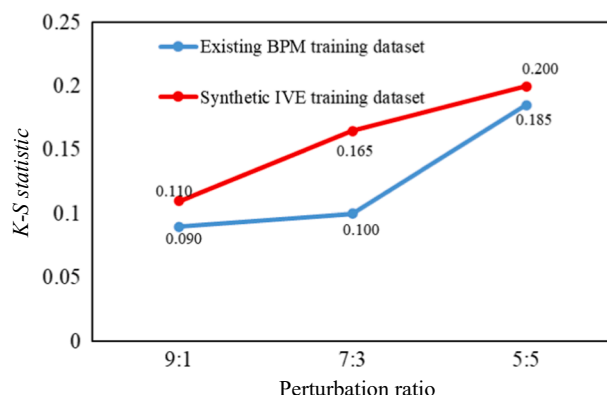


Fig. 11. K-S statistic corresponding to replacing probability of switching on with random data.

- The investigations of the sensitivity suggested that users should highly pay attention to human-building interactions especially in new design to enhance the robustness the GAN.
- Replacing the probabilities of switching on with random data was comparable with imperceptible perturbations such as patching images, which parts of original training datasets were replaced with random data. According to studies related to such perturbations [40,57], robustness of algorithms depended on characteristics and amount of random data replacing data in original datasets. If the random data (e.g., patches) lied slightly close to original datasets or too small, the random data may not impact the algorithms. Meaning the algorithms remained robust. However, if the opposite situations occurred, the algorithms may misidentify distributions of the original data (e.g., misclassifying images), causing the algorithms non-robust. The mentioned statement was relatively corresponding to the finding in the case study. In addition, types of random data played a role in influencing the robustness, which was proven by Jefferso and Marrero [71]. Nonetheless, the case study did not take the types of random data into account, where such issue may be considered in the future work.

4.3.2. Altering work area illuminance

According to the boxplots associated with $A_{\text{perturbation}}$ in Fig. 12, increases of the perturbation scales for altering the work area illuminance in both *existing BPM training dataset* and *synthetic IVE training dataset* increase uncertainty of $A_{\text{perturbation}}$. Uncertainty of $A_{\text{perturbation}}$ was notably associated with the perturbation scale. Similar to the previous case, perturbing the *synthetic IVE training dataset* have more influence on the uncertainty of $A_{\text{perturbation}}$ than perturbing the *existing BPM training dataset*.

The *p-values* in Table 7 are less than 0.05 in 5 out of 6 cases, which shows that $A_{\text{perturbation}}$ and $A_{\text{non-perturbation}}$ are significantly different in most cases. The result suggested that altering the work area illuminance significantly impact the robustness of the GAN. Additionally, altering work area illuminance in the *existing BPM training dataset* had less influence on reductions of the robustness than altering that in the *synthetic IVE training dataset*. The null hypothesis was rejected in two cases, where the perturbation scale was 30% and 50%, when the work area illuminance in the *existing BPM training dataset* was altered. However, the null hypothesis was rejected in all cases associated with the other training dataset. The finding was reasonably corresponding to what stated by Engstrom et al. [42]. They found that altering training data (e.g., rotating and translating image) significantly degraded their classifier robustness. Tramèr and Boneh [72] found similar outcomes, which were considered as the robustness trade-off.

According to Fig. 13, the *K-S statistics* associated with the *perturbed existing BPM datasets* are lower than those associated with the *perturbed synthetic IVE datasets* throughout the perturbation scales. The result suggested that the GAN was less sensitive to the *existing BPM* than the *context-aware design-specific data*.

The results of the hypothesis testing may be implicit to the significant impacts of uncertain experimental tools on the robustness and uncertainty of the GAN. The results can be the evidence for encouraging users to emphasize the importance and influence of experimental tools before conducting experiments. In practice, users are recommended to include procedures of calibrating experimental tools in experiments to reduce uncertainty that may occur in outcomes of BPMs.

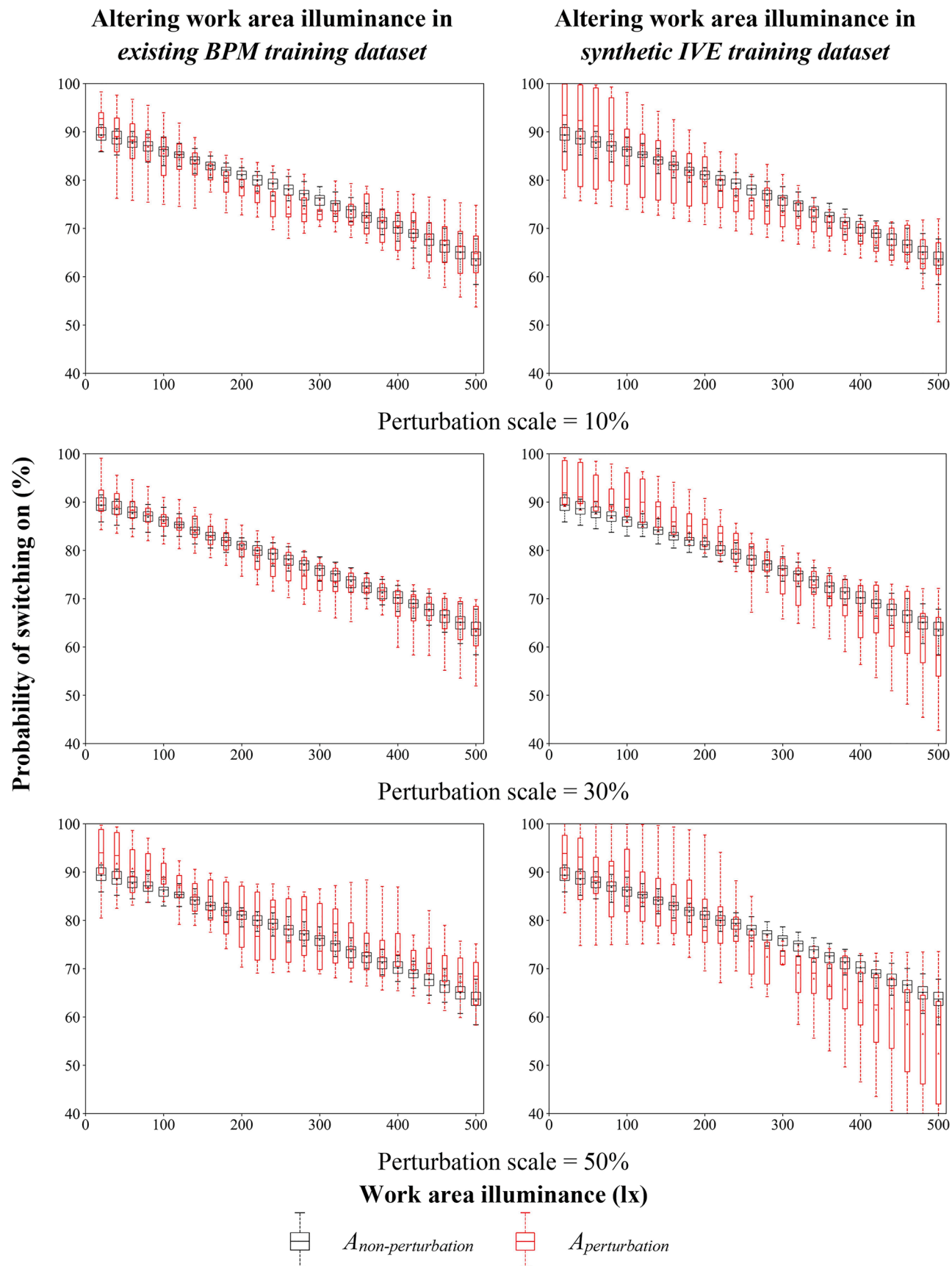
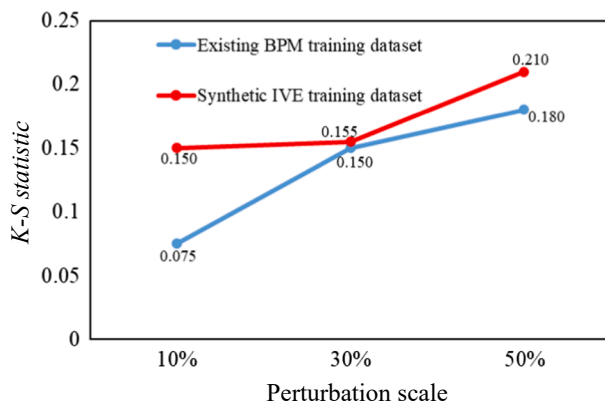


Fig. 12. Augmented BPMs corresponding to altering work area illuminance.

Table 7

P-values corresponding to altering work area illuminance.

Perturbation scale	Existing BPM training dataset		Synthetic IVE training dataset	
		P-value		P-value
10%		0.628		< 0.05
30%		< 0.05		< 0.05
50%		< 0.05		< 0.05

**Fig. 13.** K-S statistic corresponding to altering work area illuminance.

5. Limitations of the study

Major limitations of the study include:

- The case study only investigated the robustness of the GAN regarding the input parameters (i.e., the *existing BPM* and the *context-aware design-specific data*). The robustness associated with other components such as structure of the computation was excluded in the case study. Research attention on the robustness analysis of other components is needed in the future.
- The case study limited the robustness analysis with three perturbation techniques. Other techniques that may have impacts on the robustness should be investigated to be able to draw comprehensive discussions.
- More perturbation levels and smaller intervals should be considered to investigate the robustness. Due to limitations of resources (e.g., computational costs and times) and purposes of the case study, the perturbation was limited to large intervals between low and high perturbation levels.
- The uncertainty results were quantitatively explained. To better understand and use model uncertainty in the future, the uncertainty should be modeled deterministically. Unfortunately, the modeling approach was not taken into an account in this work. To enhance performance of the framework, such approach needs attention in the future research.

6. Conclusions and future work

The robustness analysis using perturbation techniques has effectively identified the robustness, uncertainty, and sensitivity related to the problem in the case study. The hypothesis tests have shown that the proposed approach allowed the investigation and comprehension of factors influencing uncertainty that impacts robustness of the GAN. Several techniques were applied to observe the influence of the perturbation and assess the robustness including adding noise, replacing data with noise, and altering data. According to the case study, adding noise relatively impacted the robustness of the GAN but not in any statistically significant manner. In addition, it marginally increased the uncertainty of the *augmented BPMs*. Replacing data in the training

datasets with noise and altering data in the training datasets caused significant reduction in the robustness of the GAN and increased the uncertainty of the *augmented BPMs*. The findings agreed with previous studies mentioning that impacts of perturbations reduced the robustness of machine learning models [49,73]. Furthermore, the GAN was more sensitive to the *context-aware design-specific data* than the *existing BPM*. Such findings may be used as a guide to create procedures of perturbations in future applications. However, other applications may give different outcomes. Applying the robustness analysis needs insight to determine which perturbation techniques and ratios should be applied along with balancing between resources, and quality of results needed.

The main purpose of the case study was to prove the effectiveness of the framework through the illustrative case study. In this paper, the authors used a lighting application for the case study, since lighting is a common case in building analysis and one of the most studied features of IVE simulations. In fact, the framework is generic, which can be applied to not only lighting studies, but other studies related to human-building interactions (e.g., thermal and acoustical comfort studies) and different BPMs. Additionally, the robustness, uncertainty, and sensitivity are dependent on several factors such as input parameters, a computational structure, and nature of a computation. This study only investigated the robustness of the computation relative to input parameters. Therefore, future research is needed to investigate other factors that may significantly impact the robustness and evaluate the framework on other applications.

In practice, designers and engineers use BPMs to estimate building performance. During the analysis, many assumptions may be made with respect to input parameters. The assumed values may differ from the actual one obtained from actual measurements. Although designers and engineers may not know the exact difference, perturbation allows them to assume potential levels of such difference. Thus, they can infer the potential impact of uncertainty associated with input parameters. In this way, robustness analysis is crucial for quantitatively understanding the uncertainty of input parameters and understanding its influence on BPMs. Designers and engineers can better understand whether BPMs are reliable and produce accurate outcomes. As a result, they gain confidence on using BPMs to assist decision-making, avoid design failures, and enhance design optimizations. Future work will address the robustness of other machine learning approaches [74–78] when applied to building performance modeling.

Declaration of Competing Interest

The authors declare that they have no known competing financial interests or personal relationships that could have appeared to influence the work reported in this paper.

Acknowledgements

This paper was partially supported by the U.S. National Science Foundation Award #1640818. Any opinions, findings, and conclusions or recommendations expressed in this material are those of the author(s) and do not necessarily reflect the views of the National Science Foundation.

References

- [1] C. Atici, Carbon emissions in central and eastern Europe: environmental kuznets curve and implications for sustainable development, *Sustain. Develop.* 17 (3) (2009) 155–160, <https://doi.org/10.1002/sd.372>.
- [2] B.V. Venkatarama Reddy, Sustainable materials for low carbon buildings, *Int. J. Low-Carbon Technol.* 4 (3) (2009) 175–181, <https://doi.org/10.1093/ijlct/ctp025>.
- [3] R. Evins, A review of computational optimisation methods applied to sustainable building design, *Renew. Sustain. Energy Rev.* 22 (2013) 230–245, <https://doi.org/10.1016/j.rser.2013.02.004>.
- [4] S. Saeidi, G. Rentalia, T. Rizzato, T. Hong, N. Johannsen, Y. Zhu, Exploring thermal state in mixed immersive virtual environments, *J. Build. Eng.* 44 (June) (2021), 102918, <https://doi.org/10.1016/j.jobe.2021.102918>.

[5] C. Chokwithaya, Y. Zhu, R. Dibiano, S. Mukhopadhyay, Combining context-aware design-specific data and building performance models to improve building performance predictions during design, *Autom. Constr.* 107 (2019), 102917, <https://doi.org/10.1016/j.autcon.2019.102917>.

[6] S. Norouziasl, A. Jafari, Y. Zhu, Modeling and simulation of energy-related human-building interaction: a systematic review, *J. Build. Eng.* 44 (June) (2021), 102928, <https://doi.org/10.1016/j.jobe.2021.102928>.

[7] H.T. Pao, Comparing linear and nonlinear forecasts for Taiwan's electricity consumption, *Energy* 31 (12) (2006) 1793–1805, <https://doi.org/10.1016/j.energy.2005.08.010>.

[8] M. Aydinapal, V.I. Ugursal, A.S. Fung, Modeling of the space and domestic hot-water heating energy-consumption in the residential sector using neural networks, *Appl. Energy* 79 (2) (2004) 159–178, <https://doi.org/10.1016/j.apenergy.2003.12.006>.

[9] B. Blocken, C. Gualtieri, Ten iterative steps for model development and evaluation applied to computational fluid dynamics for environmental fluid mechanics, *Environ. Modell. Software* 33 (2012) 1–22, <https://doi.org/10.1016/j.envsoft.2012.02.001>.

[10] C. Chokwithaya, Y. Zhu, R. Dibiano, M. Supratik, A machine learning algorithm to improve building performance modeling during design, *MethodsX* 7 (2020) 35–49, <https://doi.org/10.1016/j.mex.2019.10.037>.

[11] J.A. Love, Manual switching patterns in private offices, *Light. Res. Technol.* 30 (1) (1998) 45–50, <https://doi.org/10.1177/096032719803000107>.

[12] A.T. Nguyen, S. Reiter, P. Rigo, A review on simulation-based optimization methods applied to building performance analysis, *Appl. Energy* 113 (2014) 1043–1058, <https://doi.org/10.1016/j.apenergy.2013.08.061>.

[13] B. Si, J. Wang, X. Yao, X. Shi, X. Jin, X. Zhou, Multi-objective optimization design of a complex building based on an artificial neural network and performance evaluation of algorithms, *Adv. Eng. Inf.* 40 (March) (2019) 93–109, <https://doi.org/10.1016/j.aei.2019.03.006>.

[14] P. De Wilde, C. Martinez-Ortiz, D. Pearson, I. Beynon, M. Beck, N. Barlow, Building simulation approaches for the training of automated data analysis tools in building energy management, *Adv. Eng. Inf.* 27 (4) (2013) 457–465, <https://doi.org/10.1016/j.aei.2013.05.001>.

[15] V. Asghari, Y.F. Leung, S.C. Hsu, Deep neural network based framework for complex correlations in engineering metrics, *Adv. Eng. Inf.* 44 (February) (2020), 101058, <https://doi.org/10.1016/j.aei.2020.101058>.

[16] X. Yang, W. Chen, A. Li, C. Yang, Z. Xie, H. Dong, BA-PNN-based methods for power transformer fault diagnosis, *Adv. Eng. Inform.* 39 (2019) 178–185, <https://doi.org/10.1016/j.aei.2019.01.001>.

[17] G.H. Kruger, A.J. Shih, D.G. Hattingh, T.I. Van Niekerk, Intelligent machine agent architecture for adaptive control optimization of manufacturing processes, *Adv. Eng. Inf.* 25 (4) (2011) 783–796, <https://doi.org/10.1016/j.aei.2011.08.003>.

[18] R. Pasquier, I.F.C. Smith, Robust system identification and model predictions in the presence of systematic uncertainty, *Adv. Eng. Inf.* 29 (4) (2015) 1096–1109, <https://doi.org/10.1016/j.aei.2015.07.007>.

[19] M. Manfren, N. Aste, R. Moshksar, Calibration and uncertainty analysis for computer models - meta-model based approach for integrated building energy simulation, *Appl. Energy* 103 (2013) 627–641, <https://doi.org/10.1016/j.apenergy.2012.10.031>.

[20] C.J. Hopfe, J.L.M. Hensen, Uncertainty analysis in building performance simulation for design support, *Energy Build.* 43 (10) (2011) 2798–2805, <https://doi.org/10.1016/j.enbuild.2011.06.034>.

[21] M. Weisberg, Robustness analysis, in: The 2004 Biennial Meeting of The Philosophy of Science Association, vol. 73, no. 5, 2006, pp. 730–742, <https://www.jstor.org/stable/10.1086/518628>.

[22] J.C. Helton, J.D. Johnson, W.L. Oberkampf, C.J. Sallaberry, Representation of analysis results involving aleatory and epistemic uncertainty, *Int. J. Gen. Syst.* 39 (6) (2010) 605–646, <https://doi.org/10.1080/03081079.2010.486664>.

[23] H. Bae, R.V. Grandhi, R.A. Canfield, Epistemic uncertainty quantification techniques including evidence theory for large-scale structures, *Comput. Struct.* 82 (13–14) (2004) 1101–1112, <https://doi.org/10.1016/j.compstruc.2004.03.014>.

[24] G.B. Drummond, S.L. Vowler, Variation: Use it or misuse it - replication and its variants, *J. Physiol.* 590 (11) (2012) 2539–2542, <https://doi.org/10.1113/j.physiol.2012.234260>.

[25] C. Chokwithaya, Y. Zhu, A. Jafari, Applying the Gaussian mixture model to generate large synthetic data from a small data set, in: Construction Research Congress, 2020, pp. 1251–1260, doi: 10.1061/9780784482865.132.

[26] A. Mehrtash, W.M. Wells, C.M. Tempany, P. Abolmaesumi, T. Kapur, Confidence calibration and predictive uncertainty estimation for deep medical image segmentation, *ArXiv* 39 (12) (2019) 3868–3878, <https://doi.org/10.1109/tnmi.2020.3006437>.

[27] J. Moon, J. Kim, Y. Shin, S. Hwang, Confidence-aware learning for deep neural networks, *arXiv*, 2020.

[28] D.J.C. MacKay, A practical Bayesian framework for back propagation networks, *Neural Comput.* 4 (1992) 448–472.

[29] A. Graves, Practical variational inference for neural networks, in: 25th Annual Conference on Neural Information Processing Systems, 2011, pp. 1–9.

[30] R.M. Neal, Bayesian learning for neural networks (Lecture Notes in Statistical Vol. 118), 1997.

[31] Y. Gal, Z. Ghahramani, Dropout as a Bayesian approximation: representing model uncertainty in deep learning, in: International Conference on Machine Learning, 2016, pp. 1050–1059.

[32] S.M.M. Dezfouli, A. Fawzi, O. Fawzi, P. Frossard, S. Soatto, Robustness of classifiers to universal perturbations: a geometric perspective, in: 6th International Conference on Learning Representations, 2018, pp. 1–15.

[33] A. Rozsa, M. Günther, E.M. Rudd, T.E. Boult, Facial attributes: accuracy and adversarial robustness, *Pattern Recogn. Lett.* 124 (2019) 100–108, <https://doi.org/10.1016/j.patrec.2017.10.024>.

[34] A. Fawzi, O. Fawzi, P. Frossard, Analysis of classifiers' robustness to adversarial perturbations, *Machine Learn.* 107 (3) (2018) 481–508, <https://doi.org/10.1007/s10994-017-5663-3>.

[35] V. Tyagi, C. Welleke, On desensitizing the mel-cepstrum to spurious spectral components for robust speech recognition, in: *IEEE International Conference on Acoustics, Speech and Signal Processing*, 2004, pp. 1–9, <https://doi.org/10.1109/ICASSP.2005.1415167>.

[36] M. Cisse, Y. Adi, N. Neverova, J. Keshet, Houdini: Fooling deep structured visual and speech recognition models with adversarial examples, in: *Advances in Neural Information Processing Systems*, 2017, pp. 6978–6988.

[37] C. Chokwithaya, Y. Zhu, S. Mukhopadhyay, E. Collier, Augmenting building performance predictions during design using generative adversarial networks and immersive virtual environments, *Autom. Constr.* 119 (2020), 103350, <https://doi.org/10.1016/j.autcon.2020.103350>.

[38] C. Struck, P.J.C.J. de Wilde, C.J. Hopfe, J.L.M. Hensen, An investigation of the option space in conceptual building design for advanced building simulation, *Adv. Eng. Inf.* 23 (4) (2009) 386–395, <https://doi.org/10.1016/j.aei.2009.06.004>.

[39] A. Jungo, R. Meier, E. Ermis, M. Blatti-Moreno, E. Herrmann, R. Wiest, M. Reyes, On the effect of inter-observer variability for a reliable estimation of uncertainty of medical image segmentation, in: *International Conference on Medical Image Computing and Computer-Assisted Intervention*, 2018, pp. 682–690, https://doi.org/10.1007/978-3-030-00928-1_77.

[40] D. Karmon, D. Zoran, Y. Goldberg, LaVAN: Localized and visible adversarial noise, in: *35th International Conference on Machine Learning*, 2018, vol. 6, pp. 2507–2515.

[41] D. Kang, Y. Sun, D. Hendrycks, T. Brown, J. Steinhardt, Testing robustness against unforeseen adversaries, 2019, [http://arxiv.org/abs/1908.08016](https://arxiv.org/abs/1908.08016).

[42] L. Engstrom, B. Tran, D. Tsipras, L. Schmidt, A. Madry, Exploring the landscape of spatial robustness, in: *36th International Conference on Machine Learning*, 2019, pp. 1802–1811.

[43] N. Carlini, D. Wagner, Audio adversarial examples: Targeted attacks on speech-to-text, in: *2018 IEEE Symposium on Security and Privacy Workshops*, 2018, pp. 1–7, doi: 10.1109/SPW.2018.00009.

[44] Y. Qin, N. Carlini, I. Goodfellow, G. Cottrell, C. Raffel, Imperceptible, robust, and targeted adversarial examples for automatic speech recognition, in: *36th International Conference on Machine Learning*, 2019, pp. 5231–5240.

[45] M. Alzantot, B. Balaji, M. Srivastava, Did you hear that? Adversarial examples against automatic speech recognition, 2018, pp. 1–6, [http://arxiv.org/abs/1801.00554](https://arxiv.org/abs/1801.00554).

[46] R. Jia, P. Liang, Adversarial examples for evaluating reading comprehension systems, in: *Conference on Empirical Methods in Natural Language Processing*, 2017, pp. 2021–2031, <https://doi.org/10.18653/v1/d17-1215>.

[47] W. Thomas, R.D. Cook, Assessing influence on predictions from generalized linear models, *Technometrics* 32 (1) (1990) 59–65, <https://doi.org/10.1080/0041706.1990.10484593>.

[48] A. Haghnegahdar, S. Razavi, Insights into sensitivity analysis of earth and environmental systems models: on the impact of parameter perturbation scale, *Environ. Modell. Software* 95 (2017) 115–131, <https://doi.org/10.1016/j.envsoft.2017.03.031>.

[49] A. Fawzi, S.M. Moosavi-Dezfooli, P. Frossard, The robustness of deep networks: a geometrical perspective, *IEEE Signal Process Mag.* 34 (6) (2017) 50–62.

[50] Y.-C. Hsu, Z. Kira, Neural network-based clustering using pairwise constraints, 2015, pp. 1–12, [http://arxiv.org/abs/1511.06321](https://arxiv.org/abs/1511.06321).

[51] H. Hosseini, B. Xiao, R. Poovendran, Google's cloud vision API is not robust to noise, in: *16th IEEE International Conference on Machine Learning and Applications*, 2017, pp. 101–105, <https://doi.org/10.1109/ICMLA.2017.0-172>.

[52] G.J. Barlow, C.K. Oh, Robustness analysis of genetic programming controllers for unmanned aerial vehicles, in: *Genetic and Evolutionary Computation Conference*, vol. 1, 2006, pp. 135–142, doi: 10.1145/1143997.1144023.

[53] B. Li, C. Chen, W. Wang, L. Carin, Certified adversarial robustness with additive noise, *Advances in Neural Information Processing Systems*, 2018, pp. 1–15, [http://arxiv.org/abs/1809.03113](https://arxiv.org/abs/1809.03113).

[54] M. Ahmadlou, H. Adeli, Enhanced probabilistic neural network with local decision circles: a robust classifier, *Integr. Comput.-Aided Eng.* 17 (3) (2010) 197–210, <https://doi.org/10.3233/ICA-2010-0345>.

[55] D. Rolnick, A. Veit, S. Belongie, N. Shavit, Deep learning is robust to massive label noise, 2017, pp. 1–10, [http://arxiv.org/abs/1705.10694](https://arxiv.org/abs/1705.10694).

[56] W. Liu, W. Lin, Additive white gaussian noise level estimation in SVD domain for images, *IEEE Trans. Image Process.* 22 (3) (2013) 872–883, <https://doi.org/10.1109/TIP.2012.2219544>.

[57] A. Liu, X. Liu, J. Fan, Y. Ma, A. Zhang, H. Xie, D. Tao, Perceptual-sensitive GAN for generating adversarial patches, in: *the AAAI Conference on Artificial Intelligence*, 2019, vol. 33, pp. 1028–1035, doi: 10.1609/aaai.v33i01.33011028.

[58] C. Chokwithaya, E. Collier, Y. Zhu, S. Mukhopadhyay, Improving prediction accuracy in building performance models using generative adversarial networks (GANs), in: *International Joint Conference on Neural Networks*, 2019, pp. 1–9, <https://doi.org/10.1109/IJCNN.2019.8852411>.

[59] D.R.G. Hunt, Predicting artificial lighting use- a method based upon observed patterns of behavior, *Light. Res. Technol.* 12 (1) (1980) 7–14, <https://doi.org/10.1177/096032718001200102>.

[60] S. Saeidi, C. Chokwithaya, Y. Zhu, M. Sun, Spatial-temporal event-driven modeling for occupant behavior studies using immersive virtual environments,

Autom. Constr. 94 (2018) 371–382, <https://doi.org/10.1016/j.autcon.2018.07.019>.

[61] C. Chokwitthaya, R. Dibiano, S. Saeidi, S. Mukhopadhyay, Y. Zhu, Enhancing the prediction of artificial lighting control behavior using virtual reality (VR): a pilot study, in: Construction Research Congress, 2018, pp. 216–233, doi: 10.1061/9780784481301.022.

[62] Y. Zhu, S. Saeidi, T. Rizzato, A. Roetzel, R. Kooima, Potential and challenges of immersive virtual environments for occupant energy behavior modeling and validation: a literature review, J. Build. Eng. 19 (2018) 302–319, <https://doi.org/10.1016/j.jobe.2018.05.017>.

[63] I. Goodfellow, J. Pouget-Abadie, M. Mirza, B. Xu, D. Warde-Farley, S. Ozair, A. Courville, Y. Bengio, Generative adversarial nets, in: Advances in Neural Information Processing Systems, 2014, pp. 2672–2680.

[64] P.C. Da Silva, V. Leal, M. Andersen, Occupants interaction with electric lighting and shading systems in real single-occupied offices: Results from a monitoring campaign, Build. Environ. 64 (2013) 152–168, <https://doi.org/10.1016/j.buildenv.2013.03.015>.

[65] C.M. Bishop, Pattern recognition and machine learning. Springer, 2006, ISBN 13: 9780387310732; ISBN 10: 0387310738.

[66] X.Y. Sun, L.T.H. Newham, B.F.W. Croke, J.P. Norton, Three complementary methods for sensitivity analysis of a water quality model, Environ. Modell. Software 37 (2012) 19–29, <https://doi.org/10.1016/j.envsoft.2012.04.010>.

[67] B. Moaveni, J.P. Conte, F.M. Hemez, Uncertainty and sensitivity analysis of damage identification results obtained using finite element model updating, Comput.-Aided Civ. Infrastruct. Eng. 24 (5) (2009) 320–334, <https://doi.org/10.1111/j.1467-8667.2008.00589.x>.

[68] F.J. Massey, The Kolmogorov-Smirnov test for goodness of fit, J. Am. Stat. Assoc. 46 (253) (1951) 68–78.

[69] L. Wang, P. Mathew, X. Pang, Uncertainties in energy consumption introduced by building operations and weather for a medium-size office building, Energy Build. 53 (2012) 152–158, <https://doi.org/10.1016/j.enbuild.2012.06.017>.

[70] R. Munir, Robustness analysis of selective image encryption algorithm based on arnold cat map permutation, in: 3rd Makassar International Conference on Electrical Engineering and Informatics, 2012, pp. 1–5.

[71] B. Jefferson, C.O. Marrero, Robust assessment of real-world adversarial examples, ArXiv Preprint ArXiv:1911.10435, 2020, pp. 1–10, <http://arxiv.org/abs/1911.10435>.

[72] A. Zwanenburg, S. Leger, L. Agolli, K. Pilz, E.G.C. Troost, C. Richter, S. Löck, Assessing robustness of radiomic features by image perturbation, 2019, doi: 10.1038/s41598-018-36938-4.

[73] D. Hendrycks, T. Dietterich, Benchmarking neural network robustness to common corruptions and perturbations, in: International Conference on Learning Representations, 2019, pp. 1–16.

[74] S. Basu, S. Ganguly, S. Mukhopadhyay, R. DiBiano, M. Karki, R. Nemani, “DeepSat,” The 23rd SIGSPATIAL International Conference on Advances in Geographic Information Systems, 2015, pp. 1–10, doi: 10.1145/2820783.2820816.

[75] S. Basu, M. Karki, S. Ganguly, R. DiBiano, S. Mukhopadhyay, S. Gayaka, R. Kannan, R. Nemani, Learning sparse feature representations using probabilistic quadtree and deep belief nets, Neural Process. Lett. 45 (3) (2017) 855–867, <https://doi.org/10.1007/s11063-016-9556-4>.

[76] Q. Liu, S. Mukhopadhyay, Unsupervised Learning using Pretrained CNN and Associative Memory Bank, in: the International Joint Conference on Neural Networks, 2018, vol. 2018-July, doi: 10.1109/IJCNN.2018.8489408.

[77] E. Collier, R. Dibiano, S. Mukhopadhyay, CactusNets: Layer Applicability as a Metric for Transfer Learning, in: the International Joint Conference on Neural Networks, 2018, vol. 2018-July, doi: 10.1109/IJCNN.2018.8489649.

[78] E. Collier, K. Duffy, S. Ganguly, G. Madanguit, S. Kalia, G. Shreekanth, R. Nemani, A. Michaelis, S. Li, A. Ganguly, S. Mukhopadhyay, Progressively growing generative adversarial networks for high resolution semantic segmentation of satellite images, in: IEEE International Conference on Data Mining Workshops, 2018, pp. 763–769, <https://doi.org/10.1109/ICDMW.2018.00115>.